NASA/TM—1999-209386

Internal Plasma Properties and Enhanced Performance of an 8-cm Ion Thruster Discharge

John E. Foster and Michael J. Patterson
Glenn Research Center, Cleveland, Ohio

National Aeronautics and
Space Administration

Glenn Research Center

October 1999

Acknowledgments

The authors would like to thank Jim Sovey for meaningful discussions regarding to this work and technicians Erhard Hartman, Mike Pastel, and Ralph Jacko for fabrication of hardware used in this investigation.

Available from

NASA Center for Aerospace Information
7121 Standard Drive
Hanover, MD 21076
Price Code: A03

National Technical Information Service
5285 Port Royal Road
Springfield, VA 22100
Price Code: A03

Internal Plasma Properties and Enhanced Performance of an 8-cm Ion Thruster Discharge

John E. Foster and Michael J. Patterson
National Aeronautics and Space Administration
Glenn Research Center
Cleveland, Ohio 44135

Summary

There is a need for a lightweight, low power ion thruster for space science missions. Such an ion thruster is under development at NASA Glenn Research Center. In an effort to better understand the discharge performance of this thruster, a version of this thruster with an anode containing electrically isolated electrodes at the cusps was fabricated and tested. Discharge characteristics of this ring cusp ion thruster were measured without ion beam extraction. Discharge current was measured at collection electrodes located at the cusps and at the anode body itself. Discharge performance and plasma properties were measured as a function of discharge power, which was varied between 20 and 50 W. It was found that ion production costs decreased by as much as 20 percent when the two most downstream cusp electrodes were allowed to float. Floating the electrodes did not give rise to a significant increase in discharge power even though the plasma density increased markedly. The improved performance is attributed to enhanced electron containment.

Introduction

There is a need for a low power (<0.5 kW), lightweight ion thruster for space science missions (refs. 1 to 3). Such a thruster is under development at NASA Glenn Research Center. This ion thruster, which generates an 8 cm diameter ion beam, is at present not optimized (ref. 4). Because at low input powers, the discharge power is a larger fraction of the total thruster power (sum of beam power and discharge power), minimizing the power required to generate the discharge plasma is particularly important. An essential aspect of optimizing the performance of this device is maximizing the discharge efficiency. The efficiency of an ion thruster discharge is characterized by the power required to produce a given beam current (ref. 5). This ion production cost, defined as the ratio of input discharge power to ion beam current, in general should be minimized for efficient discharge operation. This parameter depends to a large degree on how well the energetic electrons are contained and utilized in the discharge chamber.

Containment of these energetic electrons is typically achieved by using strong permanent magnets in a multipole configuration. The ring-cusp magnetic circuit is one such configuration that has been used effectively for energetic electron containment (ref. 6). This configuration consists of a series of magnet rings of alternating polarity. This arrangement produces a magnetic cusp at each magnet ring. In the ring-cusp configuration, electrons are prevented from reaching most of the discharge chamber surfaces due to strong magnetic field lines running nearly parallel to the chamber walls. Electrons with a sufficiently large velocity component parallel to the magnetic field are collected at the cusps; otherwise, they are reflected back into the discharge by the magnetic mirror force (ref. 7). The fact that most collection occurs at the center of the cusps (along a line that bisects the magnet ring) is readily observable as a discolored line on the magnets' surface or on the surface of the intervening material to which the magnets are affixed.

As the diameter of the discharge chamber is reduced, the density in the bulk plasma is likely to decrease with the relative increase in recombination surface area and the relative decrease in the ratio of the characteristic dimension of the discharge chamber to the electron ionization mean free path. Additionally, ion production costs tend to increase. Indeed, scaling down a 30 cm flight qualified thruster to the 8 cm beam diameter device under discussion here resulted in an increase in ion production costs that ranged from 60 to 110 percent (refs. 1 and 4).

Plasma production was investigated in the discharge chamber of the 8 cm ion thruster to obtain a better understanding of why the discharge losses are so large and how to reduce them. The discharge investigation was carried out with four cusp electrodes, three ion wall probes, one Langmuir probe and an ion collecting grid

which replaced the high voltage ion optics used for beam extraction. The cusp electrodes were used to measure the current distribution at the cusps as a function of operating condition. In addition, these electrodes were used to force the thruster to operate with current collecting at specified cusps thereby by allowing for external variation and subsequent optimization of the discharge.

It should be pointed out that data taken in this study is without ion beam extraction. It is well known that discharge properties change when there is beam extraction. Beam extraction tends to decrease the neutral concentration in the discharge chamber. Grid transparency to ions increases above the physical open area fraction during beam extraction thereby increasing the effective ion loss rate to the beam (ref. 8). Without beam extraction, ions are simply collected at the grid and re-enter the discharge as neutrals. However, because the physical geometry of the discharge chamber and the magnetic circuit does not change, the trends measured in the case without beam extraction should be reflected under those conditions with beam extraction. In this respect, the studies performed without beam extraction should yield much insight into plasma production mechanisms which should be applicable to thrusters with beam extraction.

Experimental Apparatus and Approach

These experiments were conducted in a 41 cm diameter by 43 cm long bell jar. The discharge chamber was mounted on a side port of the bell jar. The cryo-pumped bell jar maintained a background pressure in the high 10^{-8} Torr range. During discharge operation, the bell jar pressure never rose above 5×10^{-5} Torr.

A cross section of the 8 cm ion thruster's discharge chamber is illustrated in figure 1(a). The discharge chamber is cylindrically symmetric. The discharge chamber, 9 cm long, consists of a conical section with a cylindrical extension. A hollow cathode served as the electron source for the discharge (refs. 9 and 10). A cathode keeper electrode was not used in these tests. The discharge chamber is constructed of nonmagnetic stainless steel (0.6 mm thick). Four evenly spaced rings of samarium-cobalt (Sm_2Co_{17}) magnets of alternating polarity were spot-welded via nichrome straps to the outer surface of the discharge chamber to form the ring-cusp magnetic circuit. A plot of the discharge chamber's axial magnetic field is shown in figure 1(b). Located on the inner surface of the discharge chamber at each magnet ring was a stainless steel ring. The rings are named according to location as indicated in figure 1(a). Each ring, four in all, was electrically isolated from the anode shell via a ceramic paste and polyimide film sandwich as shown in the inset of figure 1(a). The insulating material is shadow-shielded by the anode ring so as to reduce the likelihood of a conducting layer forming between the ring and the anode shell. The mechanical and electrical connection to each ring is made via an alumina feed-thru located at the anode shell wall. The current to each cusp electrode and the anode shell was measured via a multimeter. Each cusp electrode and the anode shell could be independently switched into or out of the discharge circuit via single-pole switches. Additional details regarding the 8 cm thruster itself may be found in reference 4.

The xenon gas used to create the plasma enters the discharge chamber through the hollow cathode orifice and a gas feed plenum. For these experiments the flow rate to the cathode and the gas feed plenum was each fixed at 1 SCCM. The main plenum was oriented in the reverse-feed (directed toward the cathode) configuration to enhance propellant utilization in the discharge (see fig. 1(a)).

A single, multi-aperture molybdenum grid biased negative relative to the cathode was used to measure the ion saturation current in the plane where the thruster's ion acceleration grids would otherwise be located. The ion grid was electrically isolated from the discharge chamber by a 0.57 mm thick mica ring. The ion grid, which contains 1300 apertures, had a physical open area fraction of 0.18. This open area fraction was designed to simulate the effective open area fraction presented by the screen and accelerator grid combination used during actual beam extraction. Tantalum planar probes, located midway between each magnet ring at the surface of the anode shell, were used to measure ion current to the anode surface area between cusps. These wall probes were electrically isolated from the wall via polyimide film. The position of the probes are designated by numbers 1 to 3 as shown in figure 1(a). Located axially in the same plane of wall probe one but extending to the centerline of the discharge chamber was a tantalum, planar Langmuir probe. The Langmuir probe was located roughly 2.0 cm upstream of the ion grid. The component of the magnetic field parallel to the Langmuir probe's collection surface was roughly 50 G. The transverse field component at the wall probes was well over 300 G. Both the wall probes and the Langmuir probe had surface areas of 0.32 cm^2 each.

Experimental Results and Discussion

Operating Characteristics of the Four-Ring Discharge Chamber

One objective of this study was to analyze the allotment of discharge current to anode surfaces as a function of discharge power. From this information, it can be determined how effective the magnetic circuit was at confining the plasma and where the plasma production was taking place.

Figure 2 displays a plot of current allotments to the various cusps and the anode shell. Here the anode shell refers to the plenum and all the surfaces between the cusps. For these tests the discharge current varied between 1.0 and 2.0 A which corresponded to measured discharge voltages ranging between 20 and 30 V. As expected most of the electron current collection occurs at the cusps.

It is ideal to have most of the plasma production occurring near the ion grid. In relation to ion thruster operation, this condition assures the ion extraction optics a generous supply of ions. The cusp current distribution is a rough indicator of the location of the discharge. The discharge tends to be localized in those regions where most of the current is collected. In general, it then follows that to assure discharge localization near the grid, the majority of the discharge current must be collected at the most downstream cusps (refs. 11). In the case of the four-ring thruster, current is distributed among the various cusps with the just over 50 percent being collected at the most downstream rings. This distribution of currents is not consistent with efficient discharge operation as determined in earlier investigations of 30 cm ion thrusters (refs. 11 and 12). However, it should be pointed out that the current collected at the most downstream cusp increases more rapidly with increasing discharge power than at the other collection sites as illustrated in figure 2. This behavior appears to suggest that the discharge moves further downstream toward the ion grid with increasing discharge power.

Another interesting point illustrated in figure 2 is the amount of anode shell current collected. The net current collected at the shell never exceeded 2 percent of the total discharge current. The relatively small amount of electron current collected at the anode shell is a consequence of the transverse magnetic field between cusps which severely limits electron diffusion to the walls. It is also interesting to note that the current to the anode shell changes polarity from electron dominated to ion dominated as discharge power increases. This change in polarity is due to a relative increase in ion flux to the walls. This polarity change is attributed primarily to the electron retarding anode fall voltage which absolute value was measured to increase with increasing discharge power.

The ion wall probes, biased at cathode potential, provide direct measurement of the rate at which ions are lost to anode surfaces between cusps (anode shell). Over the power range investigated, ion current density at the wall probes in the conical section was consistently higher than that collected by the cylindrical extension wall probe (#1). Using the wall probe data, the average ion current collected at the shell in the conical section and the cylindrical extension was estimated. It was found that the average ion current collected in the conic region is over 40 percent higher than that collected in the cylindrical extension. In this respect, ion loss to the walls is dominated by collection in the conical section. Because of the conical region's close proximity to the cathode, the higher current density measured in this region may be due to a higher plasma density there.

Extractable ion current as a function of discharge power was determined by biasing the ion grid 20 V below cathode potential to achieve ion saturation. As expected, the ion current increased monatonically with increasing discharge power. A plot of ion grid current as a function of discharge power is shown in figure 3. Also shown in the plot is the ratio of the absolute value of the ion grid current to the total discharge current. The current ratio increases with increasing discharge current suggesting that the discharge electrons are being effectively utilized in the discharge. Additionally, the ratio of ion current collected at the walls as measured by the wall probes to the grid ion current was determined. This ratio was found to be roughly constant which suggests that these two ion fluxes are proportional. This finding indicates that the relative rates of ions lost to the wall and at the grid do not change with power.

The Effect of Current Re-Distribution on Discharge Performance

A series of experiments were undertaken to investigate the effect of externally varying the current allotments at each cusp. These experiments entailed forcing the current to collect at a given cusp combination by floating one or two selected cusp electrodes. For reference, in the baseline configuration no electrodes float. The forced redistribution was expected to give rise to variations in the ion production cost and the overall ion current to the ion grid.

For these experiments, the discharge performance was first assessed under conditions where one cusp electrode was removed from the discharge circuit. In all but one case did floating a single cusp electrode result in

a noticeable change in performance. This noticeable change, which resulted in an 8 percent reduction in ion production costs, occurred when the pole piece electrode was allowed to float. Similar results were observed when this electrode was allowed to float in a 30 cm ion thruster investigation (ref. 12). Larger changes in performance were observed when two of the four cusp electrodes were removed from the discharge circuit and allowed to float. Figures 4(a) and (b) illustrate the effect of current re-allotment on grid ion current and ion production costs (ratio of discharge power to grid ion current) for a number of notable configurations. The configuration in which the cone and cathode electrode cusp electrodes floated was not stable and therefore no data were collected at this condition. Additionally, the discharge could not be sustained with three cusps floating. As can be seen in figure 4(b), overall performance did improve relative to the baseline (no floating cusps) when two cusps were allowed to float. Best performance was achieved when both the pole piece and the cylinder cusp electrodes float simultaneously.

It is interesting to note that those collection electrode combinations that included the pole piece were the lowest performers. Because of its proximity to the ion grid, it may be anticipated that variations in current collected at the pole piece cusp should have a measurable effect on ion grid current. Pole piece collection may contribute to the reduction in ion current at the grid. Plasma losses to this cusp may actually deplete the plasma near the grid. Additionally, because the propellant is injected in the near vicinity of the pole piece ring, electron cross-field diffusion probably occurs at a more rapid rate there. In this respect, the pole piece cusp may have a parasitic effect on the discharge plasma local to the grid. Again, this reasoning is supported by the noticeable increase in performance when the pole piece electrode is allowed to float alone or float in combination with another cusp.

The Isolation of the Pole Piece and the Cylinder Ring

Enhanced Plasma Production.—Operation with the pole piece and cylinder cusp electrodes floating yielded a significant increase in performance relative to the baseline configuration and the many other cusp electrode configurations tested. With the discharge power remaining fairly constant, the increase in the ion grid current that results from floating the pole piece and cylinder cusp electrodes gives rise to roughly a 20 percent decrease in ion production costs relative to the baseline configuration (see fig. 4).

In order to obtain a better understanding of why this configuration performed best, Langmuir probe data was acquired. The transverse magnetic field component (parallel to probe surface, transverse to diffusion) was approximately 50 G. Though this field strength at the probe surface is significant, the ratio of the Debye length to Larmor radius is less than one; therefore, basic probe theory was used to analyze the Langmuir probe current-voltage characteristic (ref. 13). An average electron temperature was determined from the linear portion of a logarithmic plot of electron current versus probe voltage. Evidence of a second linear region associated with the high energy primaries was not clearly observed. The absence of the second linear portion in the logarithmic plot is primarily attributed to the elevated pressure in the discharge chamber and a poor signal to noise ratio in that region of the IV characteristic. Plasma density was determined from the ion saturation current using the relation:

$$\Gamma_i = 0.61 \cdot n_e \cdot e \sqrt{\frac{kT_e}{M_i}} \tag{1}$$

Here, M_i is the mass of the ion, e is the elementary charge on the electron, k is Boltzmann's constant, T_e is the electron temperature, and n_e is the plasma density. Because ion motion near the ion grid is not severely restricted by magnetic effects (B < 30 G), equation one should also be applicable to current collected there. The electron temperature was used along with the ion saturation current measured at the grid to estimate the ion density local to the grid. A plot of the ion density and the electron temperature for a series of operating conditions are illustrated in figures 5(a) and (b). The ion density significantly increases when the pole piece and cylinder electrodes float. Additionally, the electron temperature is larger under these floating conditions.

When these segments float, the measured increase in electron temperature and plasma density may be the result of enhanced energetic electron confinement which gives rise to enhanced plasma production. The cusp electrodes float at potentials around the ionization potential of xenon. Because the anode fall voltage ranged between 1.0 and 2.0 V below the plasma potential, the floating potentials of the cusp electrodes were actually well over 12 V below plasma potential. In this respect, electrons with energies up to a few volts above the ionization potential of xenon are reflected at these floating cusps back into the discharge. So then the benefit of the floating cusps becomes clear. This reflection mechanism has the effect of increasing the residence time

of the hot electrons in the discharge which in turn increases the likelihood of such electrons undergoing inelastic collisions with neutrals. Additionally, it is likely that this enhanced containment of hot electrons also gives rise to the increase in the measured electron temperature.

It is not surprising that floating the cylinder and pole piece cusp electrodes gives rise to the largest increase in discharge performance. The electrostatic "plugging" effect at the floating cusps combined with the strong transverse magnetic field between the cusps, give rise to enhanced energetic electron containment in the volume(the cylindrical extension) of the discharge chamber closest to the optics, thereby synergistically enhancing plasma production rates immediately upstream of the ion grid.

Further evidence in support of enhanced plasma production in the region between the floating cusps is provided by the wall probes. The ion current density collected at the wall probe between the two floating electrodes significantly increases when the electrodes are allowed to float. The wall probe ion current distribution also changes when the cusp electrodes float. When the cusp electrodes float, the current density is largest at the wall probe in the cylindrical extension as opposed to wall probe number three which was the largest under baseline conditions. The ion flux to the wall probes (#2 and #3) in the conic section show reductions in ion flux when the cusps float. Because the ion flux is directly proportional to the plasma density, it may be inferred that the increases in the ion current collected at wall probe #1 are due to increases in plasma density (to first order) in the region. This increase in density in this region increases the ion flux to the grid. Reductions in wall probes #2 and #3 may be a consequence shift in the discharge plasma toward the cylindrical extension.

It should also be noted that the polarity of the shell current changes from ion dominated to electron dominated when the cusp electrodes float. This finding is particularly interesting in that it suggests that the rate of electron diffusion into the shell must be increasing. This increase is most likely attributed to an increase in the energetic electron population as suggested by the increase in the electron temperature which occurs when the cusp electrodes float.

Ion losses to the boundaries

Ideal discharge chamber operation would include minimal ion loss rates to the wall with preferential drift of ions to the ion extraction optics (ref. 14). This condition can be achieved by generating the discharge plasma in the near vicinity of the optics. Floating the cusps in the cylindrical extension to a certain degree achieves that end.

An assessment of ion losses to discharge boundaries with and without the cylindrical section's cusp electrodes floating was measured using the wall probes. It is assumed that the current density determined at each probe is representative of the region local to the probe (the surface area between the cusps). The surface area in each of these regions was then multiplied by its respective current density to determine the total current lost there. The current collected in each section was added together to determine the total ion current lost to the wall. With this quantity determined, the wall ion current fraction could be determined:

$$\varphi = \frac{I_{wall}}{I_{wall} + I_{grid}} \tag{2}$$

where the ion wall fraction is defined as the ratio of the total ion current collected at anode surfaces between cusps, I_{wall}, to the sum of the ion wall current and the current collected at the ion grid, I_{grid}. It should be noted that this parameter is only an indicator of the fraction of ions lost to the walls. It does not include the ions lost to the cusps. Figure 6 illustrates the variations in this fraction as a function of discharge power. In the baseline four-ring configuration, roughly half the ions lost to the discharge chamber boundaries end up recombining at the walls. The other half is collected at the ion grid. The fact that the ion grid accounts for only 4 percent of discharge boundary surface area suggests a nonisotropic flow of ions to the boundary, preferring the optics (ref. 14). It should be pointed out that the ratio of the wall probe current to the grid current should scale as the ratio of the surface areas. Instead, the current ratio is was an order of magnitude smaller even for the ion probe closest to the grid. The discrepancy is most likely attributed to the transverse component of the magnetic field (~300 G) between the cusps which slightly magnetizes ion flow thereby reducing the flow of ions to the wall. This effect contributes to the nonisotropic flow of ions to the grid. The fraction of ions lost to the walls decreases by roughly 20 percent when the pole piece and cylinder cusps float, suggesting that this configuration further enhances the nonisotropic flow of the ions to the boundaries.

Conclusion

Discharge plasma properties of an 8 cm ion thruster without beam extraction was investigated. As expected, most of the discharge current was measured to collect at the cusps. Less than 2 percent of the discharge current is collected at the wall surfaces between cusps. Modifying the current distribution to the cusps was found to give rise changes in discharge performance. It was found that floating the pole piece and cylinder cusps gives rise to significant increases in performance as measured by increases in ion current to the grid and decreases in ion production costs. This increase in performance is believed to be due to enhanced confinement of energetic electrons by the floating potential at the floating cusps. This enhanced confinement increases the ionization efficiency of hot electrons. These findings point to a relatively straightforward way to improve performance of the 8 cm ion thruster.

References

1. Patterson, M.J., Grisnik, S.P., and Soulas, G.C., "Scaling of Ion Thrusters to Low Power," Proceedings of the 25th International Electric Propulsion Conference, Cleveland, OH, 1997, IEPC Paper 97–098.
2. Cirri, G.F., Matticari, G.F., Noci, G., Perrotta, G., Ross, M.F., and Sabbogh, J., "Low thrust ion propulsion: Development activity at Proel Tecnologie," Proceedings of the 23rd International Electric Propulsion Conference, Seattle, Washington, 1993, IEPC Paper 93–107.
3. Mueller, Juergen, "Thruster options for microspacecraft—A review and evaluation of existing hardware and emerging technologies," Proceedings of the 33rd AIAA/ASME/SAE/ASEE Joint Propulsion Conference, Seattle, WA, 1997, AIAA Paper 97–3058.
4. Patterson, M.J., "Low Power Ion Thruster Development Status," Proceedings of the 34th AIAA/ASME/SAE/ASEE Joint Propulsion Conference, Cleveland, OH, 1998, AIAA Paper 98–3347.
5. Kaufman, H., "Technology of Electron Bombardment Ion Thrusters" in Advances in Electron and Electron Physics, vol. 36, pp. 266–272, Academic Press, San Francisco, 1974.
6. Sovey, J.S., Journal of Spacecraft and Rockets, vol. 21, pp. 488–495, 1984.
7. Chen, F., Introduction to Plasma Physics, Plenum Press, New York, pp. 130–134, 1984.
8. Brophy, J.R., "Simulated Ion Thruster Operation Without Beam Extraction," AIAA, DGLR, and JSASS, 21st International Electric Propulsion Conference, Orlando, FL, 1990, AIAA Paper 90–2655.
9. Ferreira, C.M., and Delcroix, J.L., J. Appl. Phys. 49(4), 2380, 1978.
10. Mirtich, M.J., "Investigation of Hollow Cathode Performance for a 30 cm Thruster," NASA TMX–68298, 1973.
11. Beattie, J.R. and Poeshel, R.L., "Ring Cusp Ion Thrusters," Proceedings of the 17th International Electric Propulsion Conference, Tokyo, Japan, 1984, IEPC Paper 84–71.
12. Beattie, J.R. and Matossian, J.N., NASA CR–174974, 1989.
13. Swift, J.D. and Schwar, M.J.R., Electrical probes for plasma diagnostics, Chapters 1, 13, Iliffe Books, New York, 1969.
14. Kaufman, H.R., Robinson, R.S., and Frisa, L.E., AIAA Journal, vol. 22, no. 11, 1544, 1984.

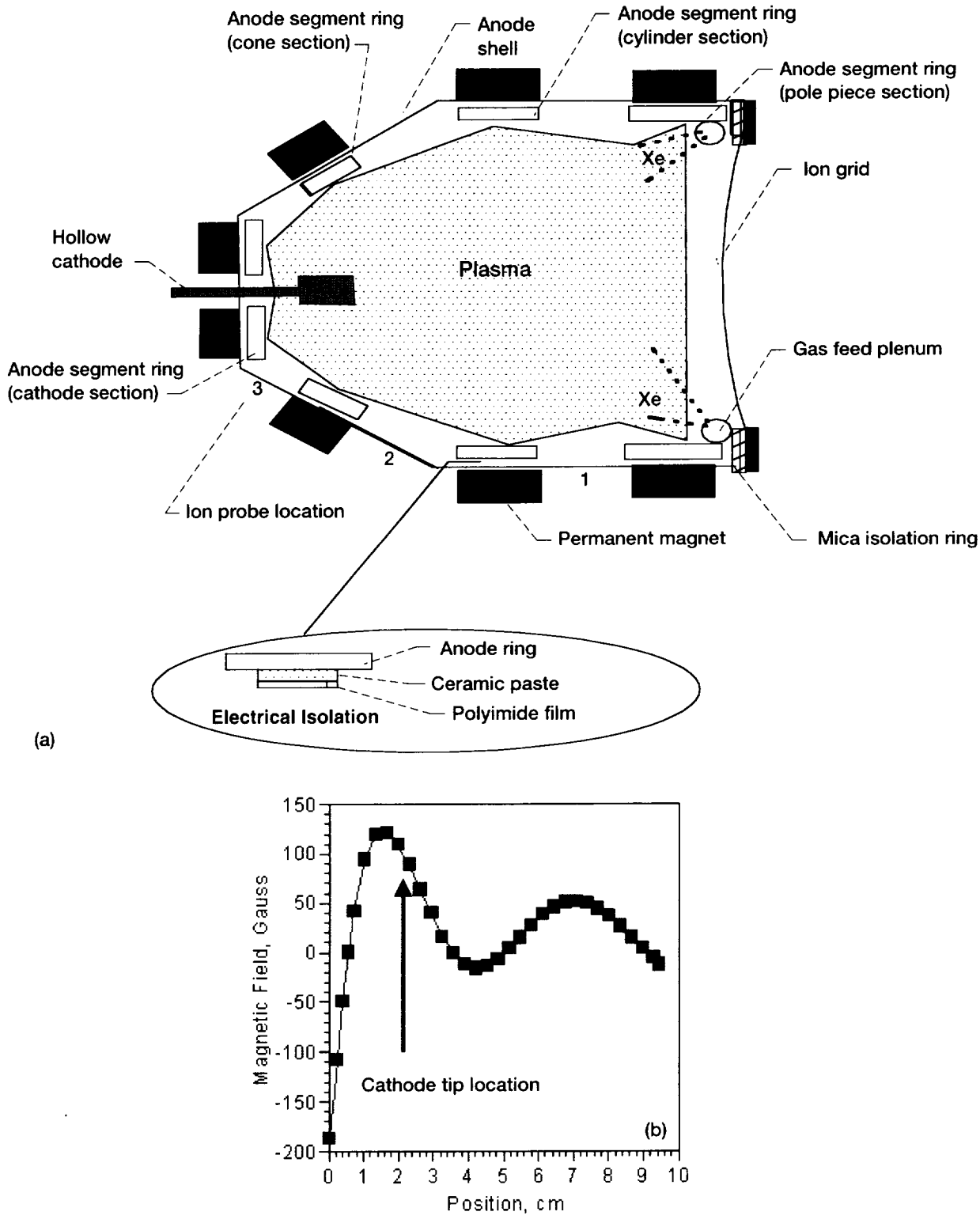

Figure 1.—Discharge chamber. (a) Segmented anode discharge chamber. Position of wall ion probes designated by numbers along discharge wall. (b) Discharge chamber axial magnetic field profile.

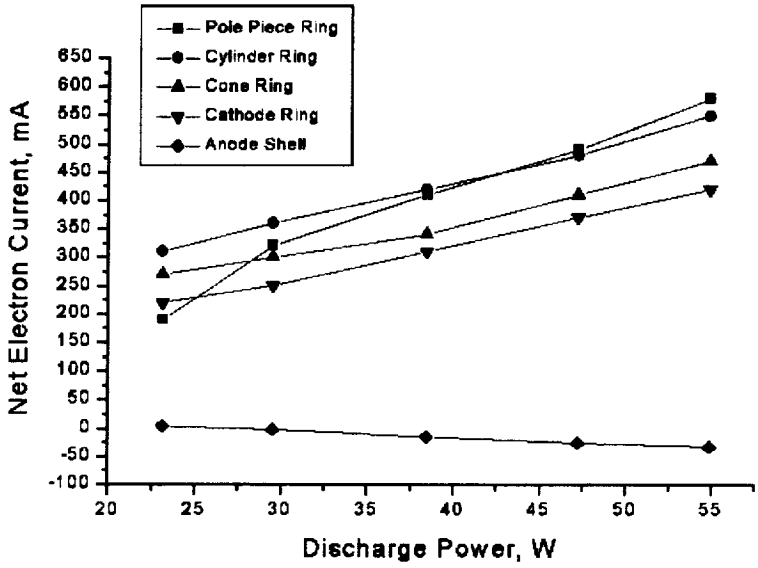

Figure 2.—Current collection at anode cusps and shell as a function of discharge power.

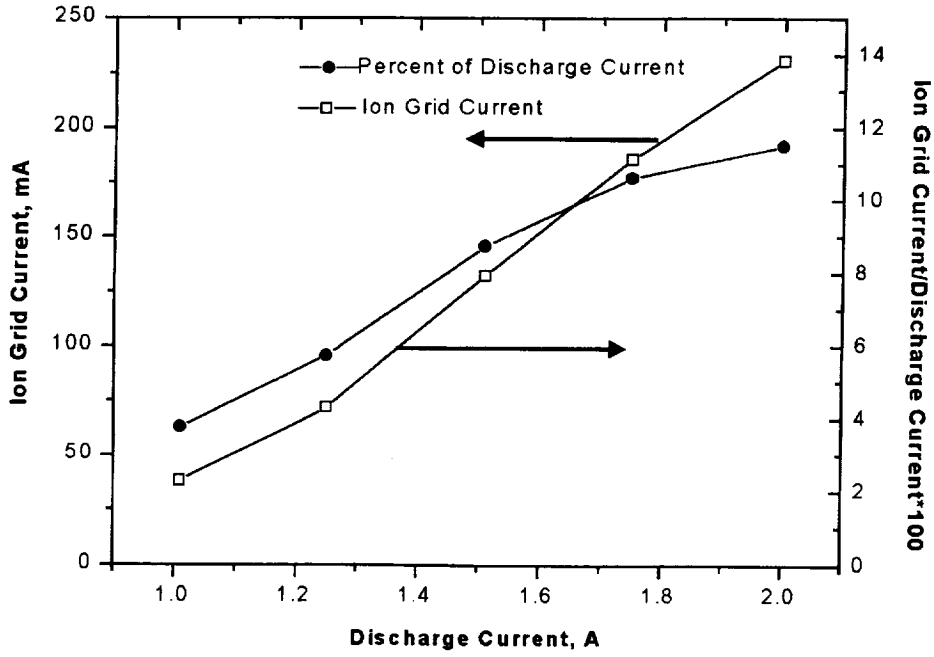

Figure 3.—Ion grid current and ion grid current fraction as a function of discharge power.

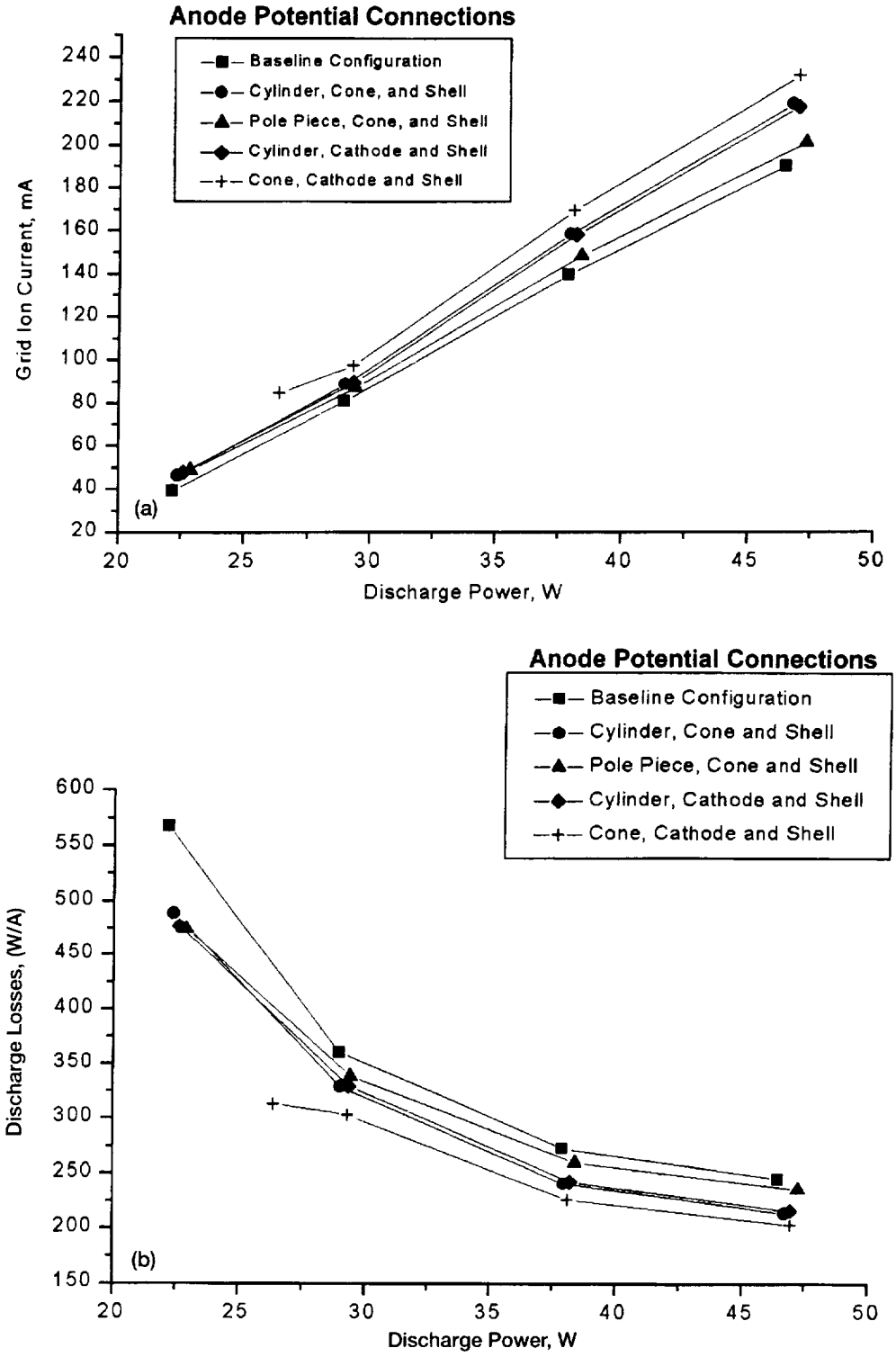

Figure 4.—(a) Ion grid current. (b) Discharge losses for a number of segment configurations as a function of discharge power.

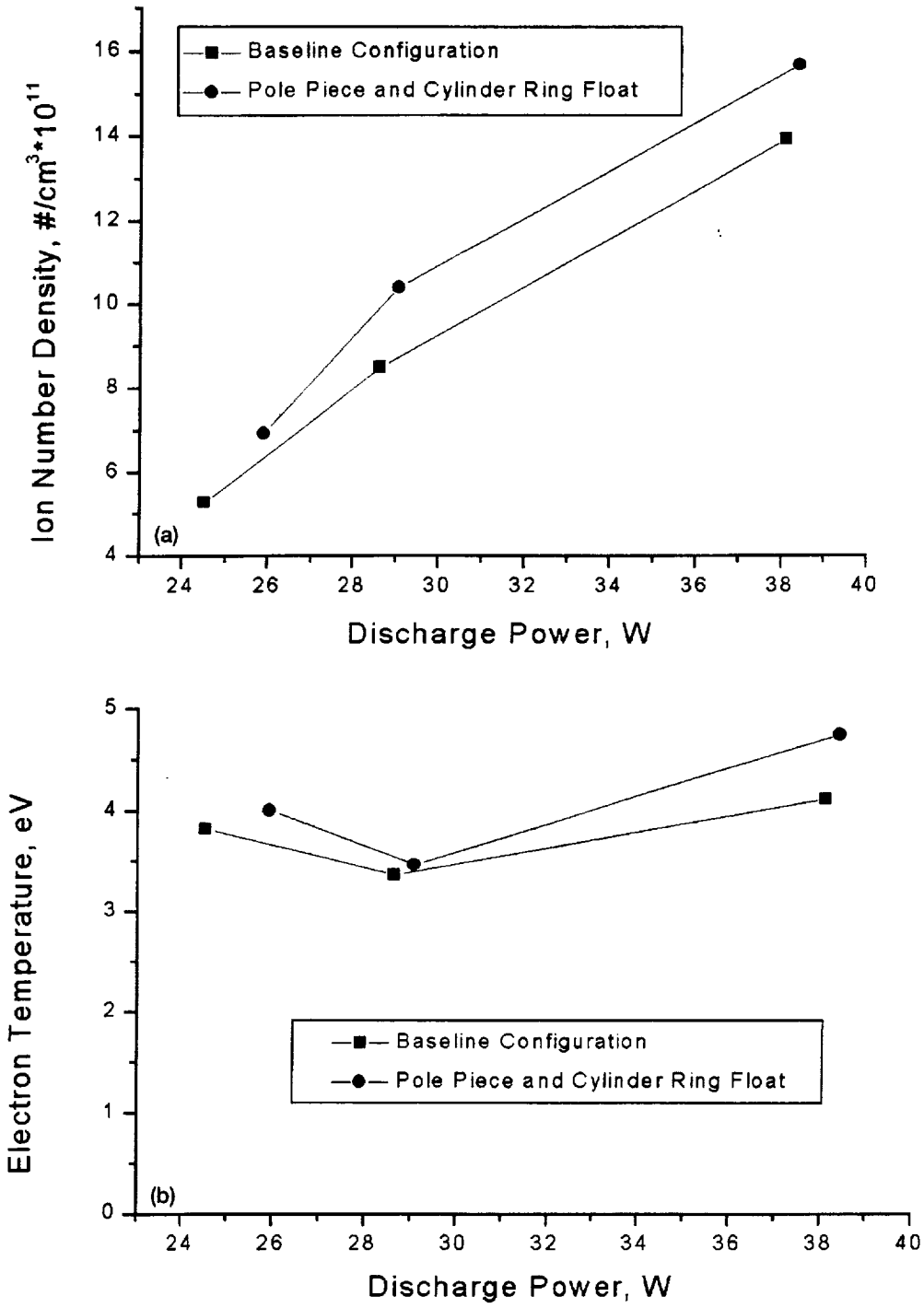

Figure 5.—Ion number density. (b) Electron temperature variations as a function of discharge power.

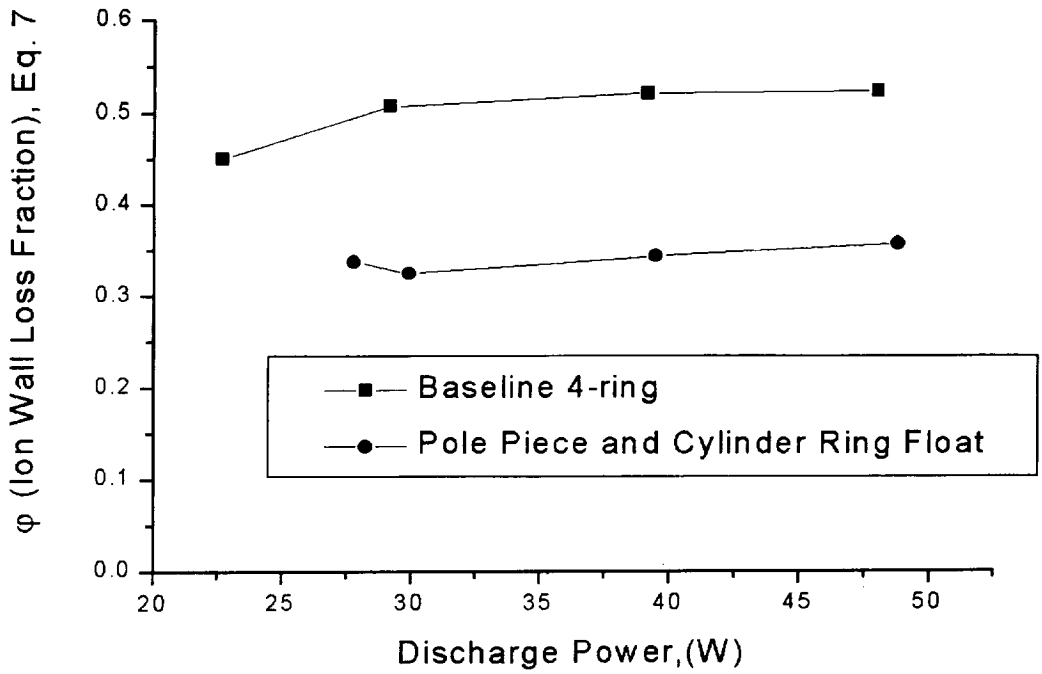

Figure 6.—Ratio of ions lost to the discharge chamber wall to total ion losses to chamber surfaces.

REPORT DOCUMENTATION PAGE

Form Approved
OMB No. 0704-0188

1. AGENCY USE ONLY (*Leave blank*)	2. REPORT DATE	3. REPORT TYPE AND DATES COVERED
	October 1999	Technical Memorandum

4. TITLE AND SUBTITLE

Internal Plasma Properties and Enhanced Performance of an 8-cm Ion Thruster Discharge

5. FUNDING NUMBERS

WU–635–1B–1B–00

6. AUTHOR(S)

John E. Foster and Michael J. Patterson

7. PERFORMING ORGANIZATION NAME(S) AND ADDRESS(ES)

National Aeronautics and Space Administration
John H. Glenn Research Center at Lewis Field
Cleveland, Ohio 44135–3191

8. PERFORMING ORGANIZATION REPORT NUMBER

E–11813

9. SPONSORING/MONITORING AGENCY NAME(S) AND ADDRESS(ES)

National Aeronautics and Space Administration
Washington, DC 20546–0001

10. SPONSORING/MONITORING AGENCY REPORT NUMBER

NASA TM—1999-209386

11. SUPPLEMENTARY NOTES

Responsible person, John E. Foster, organization code 5430, (216) 433–6131.

12a. DISTRIBUTION/AVAILABILITY STATEMENT

Unclassified - Unlimited
Subject Categories: 20 and 75 Distribution: Nonstandard

This publication is available from the NASA Center for AeroSpace Information, (301) 621–0390.

12b. DISTRIBUTION CODE

13. ABSTRACT ***(Maximum 200 words)***

There is a need for a lightweight, low power ion thruster for space science missions. Such an ion thruster is under development at NASA Glenn Research Center. In an effort to better understand the discharge performance of this thruster, a version of this thruster with an anode containing electrically isolated electrodes at the cusps was fabricated and tested. Discharge characteristics of this ring cusp ion thruster were measured without ion beam extraction. Discharge current was measured at collection electrodes located at the cusps and at the anode body itself. Discharge performance and plasma properties were measured as a function of discharge power, which was varied between 20 and 50 W. It was found that ion production costs decreased by as much as 20 percent when the two most downstream cusp electrodes were allowed to float. Floating the electrodes did not give rise to a significant increase in discharge power even though the plasma density increased markedly. The improved performance is attributed to enhanced electron containment.

14. SUBJECT TERMS

Plasma discharge; Electron bombardment; Ion engines; Confinement

15. NUMBER OF PAGES

17

16. PRICE CODE

A03

17. SECURITY CLASSIFICATION OF REPORT	18. SECURITY CLASSIFICATION OF THIS PAGE	19. SECURITY CLASSIFICATION OF ABSTRACT	20. LIMITATION OF ABSTRACT
Unclassified	Unclassified	Unclassified	